

Research

Microstructure in Zircaloy Creep Tested in the R2 Reactor

Kjell Pettersson

December 2004

SKI Perspective

Background and purpose of project

Creep of zirconium alloys in a light water reactor environment plays an important role in many situations of interest to reactor safety. During normal operation of fuel rods the external pressure will lead to creep down of the cladding so that the gap between fuel and cladding becomes closed. This is a reduction of the margin to cladding fracture in the event of a power ramp or a reactivity initiated accident. Late in life fission gas release may lead to an internal overpressure in the fuel rods which leads to outward creep and an increase of the gap between fuel and cladding. This is again an undesired condition since the increased gap means a degraded thermal conductance in the gap and a subsequent increase in the temperature of the fuel. This leads to more fission gas release and the situation is potentially unstable.

In order to have control over these different phenomena it is important to be able to calculate the amount of creep expected under various conditions. This requires reliable models for the creep deformation. It is our firm belief that the best models are based on a sound mechanistic understanding of the phenomena modelled. With regard to the irradiation creep of zirconium alloys there are a number of different proposals concerning the controlling mechanism and there is thus not yet a firm basis available for modelling irradiation creep.

The aim of the present project therefore was to improve the mechanistic understanding by characterizing the microstructure in a Zircaloy-4 guide tube which had been subjected to creep deformation in the R2 reactor in Studsvik. A unique feature of the project was that, since the tube had been deformed under bending, samples could be extracted from parts which had been deformed in tension as well as from parts deformed in compression.

Results

The SKI interest in the investigation is the need to improve the mechanistic understanding of the creep phenomena and by that improve the modelling for the safety assessment of reactor core components. An additional SKI incentive for supporting the present research is that it contributes to the development of knowledge and competence in the Swedish nuclear industry and in the institutes and university departments working with the industry.

Project information

Responsible for the project at SKI has been Jan in de Betou.
SKI Reference: 14.6-011224/01241

Research

Microstructure in Zircaloy Creep Tested in the R2 Reactor

Kjell Pettersson

Matsafe AB
Skeppargatan 84 bv
SE-114 59 Stockholm
Sweden

December 2004

This report concerns a study which has been conducted for the Swedish Nuclear Power Inspectorate (SKI). The conclusions and viewpoints presented in the report are those of the author/authors and do not necessarily coincide with those of the SKI.

Table of contents

Summary	III
Sammanfattning	IV
1. Introduction	1
2. Mechanisms of irradiation creep	2
3. Application to Zircaloy tubes	4
4. Creep results	6
5. Experimental details	6
6. Results	8
6.1 Unirradiated material	8
6.2 As-irradiated material.....	8
6.3 Irradiated and heat treated material.....	11
7. Discussion	14
8. Conclusions	16
9. References	17

Summary

Tubular specimens of Zircaloy-4 have been creep tested in bending in the R2 reactor in Studsvik. The creep deformation in the reactor core is accelerated in comparison with creep deformation outside the reactor core. The possible mechanisms behind this behaviour are described briefly. In order to determine which the actual mechanism is, the microstructure of the material creep tested in the R2 reactor has been examined by transmission electron microscopy. Due to the bending, material subjected to both tensile and compressive stress during creep was available. Since some of the proposed mechanisms might give microstructures which are different when the material is subjected to compressive or tensile stress it was assumed that examination of both types of material would give valuable information with regard to the operating mechanism.

The result of the examination was that in the as-irradiated condition there were no obvious differences detected between materials which had been deformed in tension or compression. After a heat treatment to coarsen the irradiation induced microstructure there were still no significant differences between the two types of material. However it was now observed that in addition to dislocation loops the microstructure also contained network dislocations which presumably had been invisible in the electron microscope before heat treatment due to the high density of small dislocation loops in this state. It is therefore concluded that the most probable mechanism for irradiation creep in this case is climb and glide of the network dislocations. The role of irradiation is two-fold: It accelerates climb due to the production of point defects of which more interstitials than vacancies arrive to the network dislocations stopped at an obstacles. This leads to a net climb after which a dislocation is released from the obstacle and an amount of glide takes place. The second effect is the production of loops which serve as an increasing density of obstacles to glide. The deformation rate thus decreases with irradiation dose, leading to a primary creep stage. However, finally the loop density saturates after which a steady state creep rate is established.

Sammanfattning

Prover av ledrör av Zircaloy-4 har krypprovats i R2-reaktorn i Studsvik under böj deformation. Krypningen inuti reaktorhärden är accelererad i jämförelse med krypning utanför reaktorhärden. De möjliga mekanismerna bakom detta beteende beskrivs kortfattat. För att bestämma vilken som är mekanismen har materialets mikrostruktur undersökts i transmissionselektronmikroskop. På grund av böjningen fanns i proverna material tillgängligt som deformerats både under tryckning och dragning. Eftersom en del av de föreslagna mekanismerna bör ge mikrostrukturer som skiljer sig beroende på om materialet utsatts för tryckning eller dragning antogs att studier av både typerna material borde ge intressant information om vad som varit mekanismen bakom den accelererade krypdeformationen.

Resultatet var att materialet i det bestrålade tillståndet inte uppvisade några uppenbara skillnader mellan de två typerna av material. Även efter en värmebehandling utförd för att förgrova mikrostrukturen saknades klara skillnader mellan materialen. Däremot syntes nu bland dislokations slingorna bildade vid bestrålning och värmebehandling också nätverksdislokationer som förmodligen varit osynliga i det bestrålade materialet före värmebehandlingen på grund av den höga tätheten av små dislokations slingor, som karakteriserar materialet i detta tillstånd. Därför blir slutsatsen av denna undersökning att den mest sannolika mekanismen för den accelererade krypning är klättring och glidning av nätverksdislokationerna. Bestrålningen spelar två roller. Den accelererar krypningen därför att punktdefekter bildas i stor mängd av vilka fler interstitialer än vakanser anländer till dislokationer som stoppats upp mot hinder och därför fås en klättring förbi hindren. Den andra rollen är bildningen av små dislokations slingor som fungerar som en ökande täthet av hinder för dislokationsrörelse. Töjningshasigheten avtar därför med ökande dos, man får ett skede av primärkryp. Till slut mättas dock tätheten av dislokations slingor varefter en konstant kryphastighet kommer att råda.

1. Introduction

Creep deformation, time dependent plastic deformation, may sometimes be a problem in the core of light water reactors. Normally the zirconium alloy clad fuel rods are subjected to an external pressure. This pressure causes a compressive hoop stress in the cladding which causes a slow contraction of the cladding diameter. Normally this compressive deformation is terminated when the cladding comes in contact with the fuel. Occasionally, if there for some reason is a gap in the stack of fuel pellets the creep deformation can continue and a type of cladding collapse may occur. This was a problem for a short period around 1972 but was relatively easily solved by pre-pressurizing the fuel rods so that the differential pressure was reduced. As a more long term solution more densification resistant fuel was developed. At higher burnups there is a possibility that the release of fission gases from the fuel leads to such high internal pressures in the fuel rods that the cladding is subjected to a tensile stress. It is under those circumstances important that the creep rate of the cladding is lower than the swelling rate of the fuel. Otherwise an instability situation may occur in which contact is lost between fuel and cladding. This in turn leads to an increased fuel temperature which results in release of more fission gases.

A third case of problem with creep deformation, which indirectly led to the present project, occurred recently in the Ringhals 3 and 4 reactors. In fuel bundles of a certain design higher than expected compressive forces were present on the whole bundle structure. If there was a slight initial bow of the bundle the compressive force resulted in a low bending moment on the bundle. The stresses caused by the bending moment were large enough to cause creep, a deformation which increased the bow and thus also increased the bending moment. The problem was discovered when it was noted that the control rods could not be inserted all the way when the reactor was scrammed. Due to the importance of this problem some work was devoted to looking at methods of testing the creep resistance of cladding materials in the R2 reactor in Studsvik.

A review of irradiation creep experience led to a proposal that the most suitable method for testing would be to subject fuel rods to a bending moment and measuring the resulting bow between the reactor cycles [1]. The main argument for using a bend test is that it is relatively easy to measure even very small creep strains in a bend test since also small strains result in measurable deflections of a bent rod. An additional argument for using a bend test is that it is easy to fabricate test samples from pre-irradiated cladding. This is quite important since it can be expected that the creep properties at high doses are quite different from the properties of an initially unirradiated material. The argument against using bend type specimens is that the stress distribution over the tested cross section is non-uniform. Initially the distribution over the cross section is linear from a maximum compressive stress to a maximum tensile stress of

the same magnitude. However the stress distribution may change with time depending on the creep properties of the tested material and interpretation of results may then be difficult. Fortunately all previous experience and most theoretical considerations show that the irradiation creep rate varies linearly with stress and therefore the stress distribution in a bend test stays constant during the test.

Thus a first bend type irradiation creep experiment was performed in the R2 reactor on an initially unirradiated Zircaloy-2 cladding specimen. The technical details of the test are described in [2] and the results are compared to previous creep data in [3]. The purpose of the present work has been to determine if there is anything in the microstructure of the creep tested material which might throw some light on the mechanism behind irradiation creep. One reason why this is particularly interesting in the present case is that in the creep specimen parts of the material have been subjected to a tensile stress and other parts to a compressive stress.

2. Mechanisms of irradiation creep

It is a general observation that creep deformation is faster under a fast neutron flux than it is without the neutron flux. There are a number of mechanisms proposed in order to explain this accelerating effect of the fast neutron irradiation. A review of the different mechanisms as applied to zirconium alloys can be found in the book by Franklin et. al. [4]. They distinguish between two principally different types of mechanisms, irradiation induced creep and irradiation enhanced creep. The former type of mechanisms does not exist without neutron irradiation while the latter type is an existing mechanism which is accelerated by neutron irradiation. Their classification is shown in Figure 1.

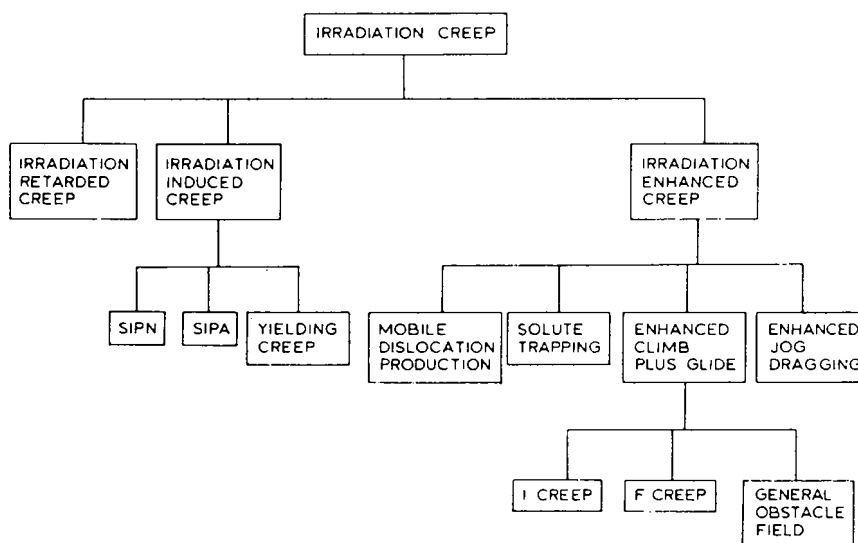


Figure 1. Classification of irradiation creep mechanisms. [4]

Note that the figure also includes a box for irradiation retarded creep. This is simply a statement of the fact that a material with an irradiation induced microstructure will creep at a slower rate than a material without. However if the material with the irradiation induced microstructure is subjected to a neutron flux it will creep faster than without the flux.

The irradiation induced microstructure in zirconium alloys irradiated at temperatures of interest for light water reactor applications, 250 – 350 °C, consists of prismatic dislocation loops of interstitial or vacancy character with an **a** ($\langle 11\bar{2}0 \rangle$) Burgers' vector. At high doses dislocations with a **c** component Burgers vector start to appear [5]. These are probably vacancy loops with a $\frac{1}{6}\langle 20\bar{2}3 \rangle$ Burgers' vector. These loops can be seen as having been formed by the removal of a disc of atoms on the basal plane. When the two faces are brought together to restore the lattice, a slight sideways motion is required in order to get a close packed configuration of atoms. Thus a vacancy loop will not normally have a $c/2$ Burgers' vector. However Griffiths states that the loops observed with a $c/2$ Burgers' vector are vacancy loops [5], so the stacking fault associated with such a loop probably has a lower energy than one would presume on the basis of intuition..

The loops play an important role in the mechanisms of irradiation induced creep. The mechanism called SIPN, for stress induced preferred nucleation, means that loops tend to nucleate with an orientation such that the material is extended in the direction of stress when the loops grow. In the mechanism termed SIPA, stress induced preferred absorption, it is assumed that there is no bias in the nucleation of loops but that the migrating defects tend to absorb at loops or edge dislocations in general with an orientation such that the material extends in the direction of stress. For both these mechanisms the strain rate is proportional to stress and neutron flux:

$$\dot{\epsilon} = C \sigma \phi \quad (1)$$

In irradiation enhanced creep the flux of defects leads to an enhancement of the creep rate. One type of model has been proposed by Gittus [6]. In Gittus' model the creep is described in terms of a balance between strain hardening and recovery in a situation where a dislocation network has developed in the material. Preferential absorption of interstitials on edge dislocations of the network leads to climb and an average coarsening of the network. This coarsening would in an unirradiated material make it possible for a few links of the network to be released and to glide and produce some strain at the same time as their glide also leads to a finer network. In the version of the model called I-creep there is a preferential absorption of interstitials because the vacancies are absorbed at other sinks, mainly voids. Thus the I-

creep model predicts a high creep rate for a material subject to void swelling which is not applicable to zirconium alloys, at least not at LWR temperatures. In the version of the model called F-creep Gittus assumes that on average an equal number of interstitials and vacancies reach edge dislocations. However by statistical fluctuations the net local arrival rate of one defect type may be non-zero and climb resulting in passage of an obstacle may occur. In general the F-creep rate is much smaller than the I-creep rate. In fact Dollins and Nichols state that Gittus has overestimated the F-creep rate by “a large factor” [7]. Their calculations on climb by statistical fluctuations results in rates one-and-a-half order of magnitude lower than experimental results. Thus the most probable form of irradiation enhanced creep is I-creep. In the absence of swelling it is assumed that edge dislocations attract vacancies more than they attract interstitials and there will thus be a net climb rate. Dollins and Nichols have estimated that a small mismatch of 0.1% would be enough to explain observed creep rates [7] in zirconium alloys.

The situation described by Gittus is one where there is a balance between strain hardening and recovery. In Zircaloy at around 300 °C such a situation is less likely to occur in recrystallized material. A more likely situation seems to be that dislocation movement is impeded by obstacles in the glide plane at stresses below the yield stress. However when irradiation starts, climb of dislocations caused by the difference in arrival rates of interstitials and vacancies, will lead to release from the obstacles and the released dislocations will glide to the next obstacle. The irradiation will lead to an increase in the number of obstacles and the creep rate will thus decrease. However the density of irradiation induced obstacles is known to saturate as evidenced by the fluence dependence of the yield strength. Thus after a certain dose the creep rate will be nearly constant and it will look as if we have the classical creep behaviour with a primary stage and a stationary secondary stage.

3. Application to Zircaloy tubes

In the present work the microstructure in a Zircaloy-4 guide tube subjected to creep deformation in bending has been examined. In order to understand what sort of microstructure to expect it is worth looking at the texture of the tube. The tube had an outer diameter of 12.4 mm and a wall thickness of 0.51 mm. The material was fully recrystallized with a grain size of about 5 μm. The texture is characterized by all grains having orientations with the basal poles in a plane perpendicular to the axial direction and oriented about ±30° from the radial direction as shown in the schematic picture in Figure 2. In a recrystallized material the $\langle 11\bar{2}0 \rangle$ poles are normally oriented in the axial direction [8].

In a tube subjected to bending the stress state is basically a uniaxial stress in the axial direction. However the magnitude of the axial stress will vary around the circumference of the

tube from a maximum tensile stress to a maximum compressive stress of the same magnitude on the opposite side of the tube.

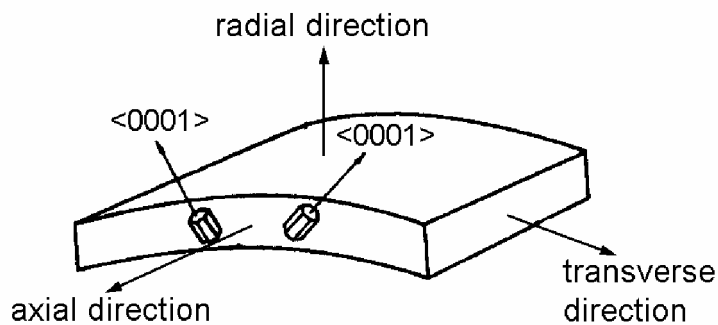


Figure 2. Schematic picture showing the most important grain orientations in a Zircaloy tube.

If deformation takes place by dislocation glide dislocations will glide on the $\langle 10\bar{1}0 \rangle$ planes which are inclined to the axial direction and the microstructure will consist of deformation dislocations and the irradiation induced loops with an **a** Burgers' vector. It is an interesting question whether or not the deformation dislocations will be visible. When examining specimens of fully recrystallized Zircaloy, which had been creep tested in the R2 reactor, no deformation dislocations at all were visible in the microstructure despite the fact that the specimens had deformed about 2-4 % [9], a deformation expected to result in a dislocation density of the order of $5 \times 10^{13} \text{ m}^{-2}$. Even if considerable recovery had occurred during irradiation it is still reasonable to expect a dislocation density of at least 10^{13} m^{-2} . It was speculated at the time that the high density of loops with an **a** Burgers' vector in some way hid the deformation dislocations. This speculation was reinforced later by Carpenter[10] who inferred from observations on the development of microstructures during irradiation in a high voltage electron microscope that in previous observations of loop structures in neutron irradiated material large loops or a dislocation network had not been visible due to the presence of the smaller **a** loops. The reason for Carpenter's conclusion was that the density of small **a** loops could not explain the observed growth strains of the material.

If on the other hand the creep deformation takes place by growth of aligned loops, extension in the axial direction can take place by interstitial loops growing on planes nearly perpendicular to the axial direction and with Burgers' vectors nearly parallel to the axial direction. Reviews on the irradiation induced microstructure in Zircaloy indicate that vacancy and interstitial loops are formed in about equal numbers at around 300 °C in what is presumably unstressed material [5]. The habit planes of the loops are normally $\langle 10\bar{1}0 \rangle$ so they are not completely prismatic. Thus one could envisage a situation when there would be a majority of interstitial loops on the tensile side and a majority of vacancy loops on the

compressive side. The question then is whether or not this could be determined by TEM since it is normally quite difficult to determine loop character when the loops are as small as they are when formed at around 300 °C [11].

4. Creep results

Two Zircaloy-4 tubes were tested for three irradiation test cycles in a hot water loop in the R2 test reactor. One of the tubes was tested out-of-flux while the other was tested inside the reactor core. The test temperature was 317 ± 1 °C. The tubes were tested in bending and the creep strain was calculated from the curvature of the specimens. The peak stress in the outer fibres of the specimens was 100 MPa. A more detailed description of the experiment can be found in [3]. The results are shown in Figure 3 as the creep strain in the outer fibre of the bent tube.

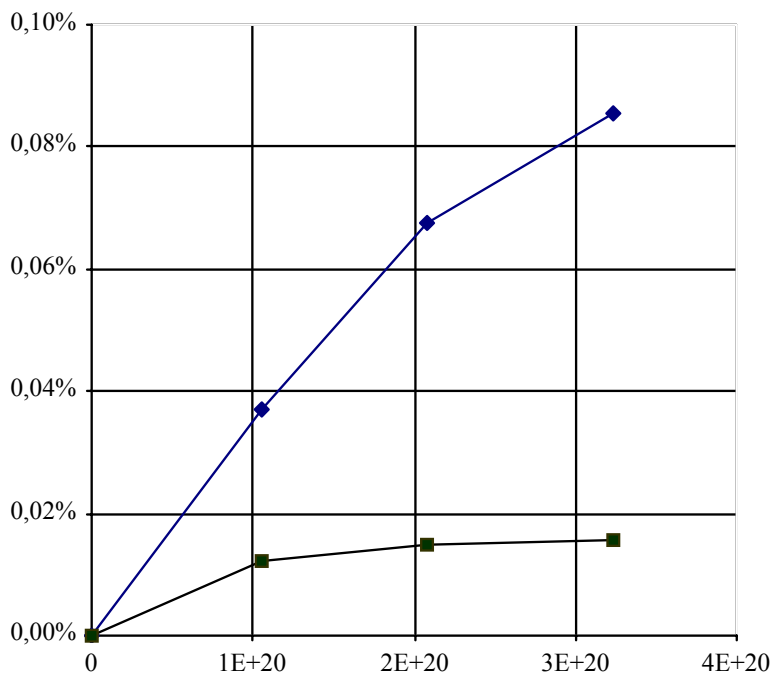


Figure 3. Creep strain as a function of fluence for the two specimens. Note that for the unirradiated specimen, the one with the lower strain, the fluence scale serves as a time scale where 10^{20} n/cm² corresponds to about 420 hours.

A comparison with other in-pile creep results compiled in [4] shows that the present results fall in the primary stage of the in-pile creep curve of the results in [4]. A further discussion of the results will follow below.

5. Experimental details

The irradiation creep specimen was marked with white paint on the outer fibre so that the location of maximum tensile stress could be identified in the later handling. A short length of the tube was cut at the location of highest fluence and specimens for TEM examination were

extracted in two different orientations, Figure 4. The reason for using two different orientations is that for cladding tubes with the $\pm 30^\circ$ texture it is impractical if not impossible to tilt a radial specimen so that the electron beam becomes parallel to the basal plane, which is necessary in order to activate the (0002) diffraction. The (0002) diffraction must be activated in order to make dislocations with an **a** Burgers' vector invisible according to the $\mathbf{b} \cdot \mathbf{g} = 0$ criterion. It is normally only when the **a** dislocations are invisible that **c** component dislocations can be identified, although in the present case no irradiation induced **c** component dislocations were expected. However occasionally a few dislocations with a **c + a** Burgers' vector may be present.

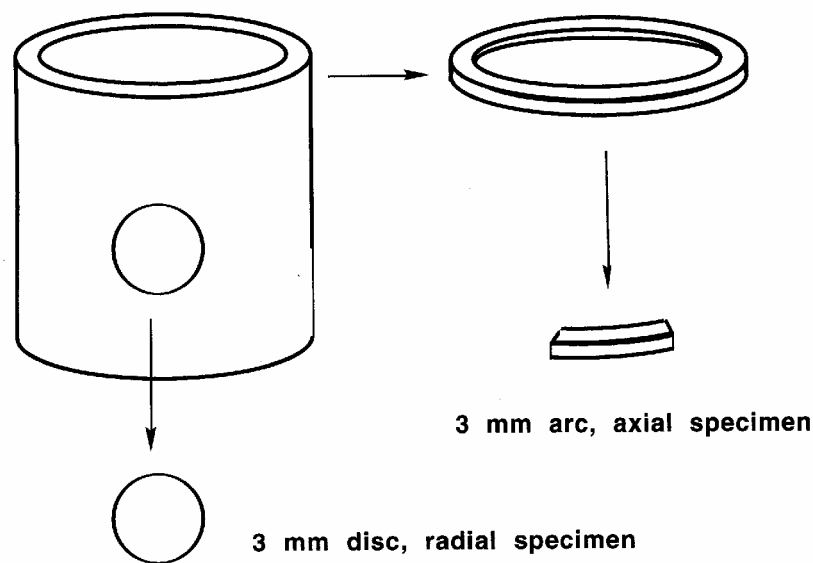


Figure 4. Specimens extracted in two different orientations. The designations "axial" and "radial" refers to the direction of the electron beam on examination of an untilted specimen in the TEM.

The specimen preparation was done by cutting rings from the cladding sample with a diamond saw. For the radial specimens the rings had a height of about 2 mm. From these rings pieces with a width of about 4 mm were cut at the locations of maximum tensile and compressive stress. These pieces were ground on both sides down to a thickness of about 0.1 mm so that the curvature was removed. After grinding a 3 mm disc was punched from the piece. Since the ring height was less than 3 mm the disc had two straight sides which during examination could serve to identify the specimen orientation in relation to the tube directions. For the axial specimens the ring was ground to a thickness of about 0.1 mm after which a length of arc of 3 mm was punched out from the ring, again at the locations of maximum tensile and compressive stress.

The specimens were thinned to electron transparency by electropolishing them in a solution of 10% perchloric acid in ethanol at a temperature of about $-26\text{ }^{\circ}\text{C}$. The specimens were examined in a JEOL 2000 EX scanning transmission electron microscope at an acceleration voltage of 200 kV. The examination work was performed with the specimens in a conventional double-tilt holder. Pictures were recorded on conventional photographic film but after development the negatives were scanned to digital form in transmission mode in a flatbed scanner and saved to hard disk for subsequent treatment.

Before electropolishing about half of the specimen blanks were heat treated at $450\text{ }^{\circ}\text{C}$ for 2 hours in order to make the loop structure coarser.

6. Results

6.1 Unirradiated material

The dislocation density in the unirradiated material was a little bit higher than expected as can be seen in Figure 5.

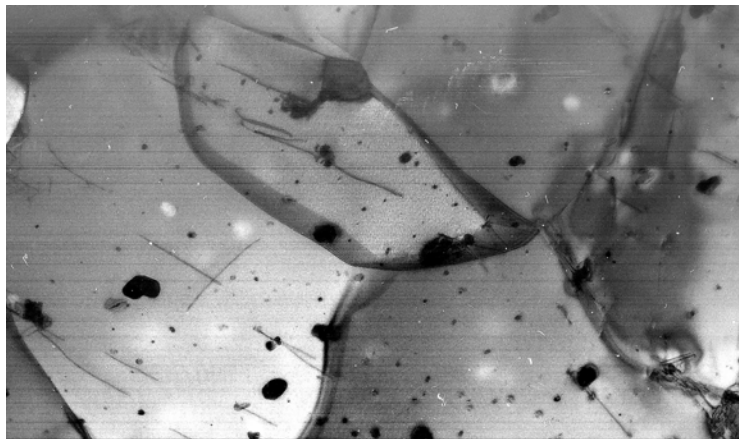


Figure 5. Microstructure in the unirradiated material. 8000x.

Counting intersections with the foil surface or measuring the line length in the picture results in a dislocation density of the order of 10^{12} m^{-2} . Figure 5 was taken with a foil with the electron beam in the radial direction. The straight dislocation segments seem to lie on the prism $\{10\bar{1}0\}$ planes. In a foil with axial orientation examination of grains with (0002) diffraction activated did not show any dislocations, which indicates, as expected, that all dislocations seen in the material have an **a** Burgers' vector.

6.2 As-irradiated material

In the irradiated material the microstructure was characterized by the typical black dot structure frequently observed in Zircaloy irradiated at temperatures around $300\text{ }^{\circ}\text{C}$. There was

no obvious difference between material which had been deformed in tension or compression. Examples of the microstructures are shown in Figure 6.

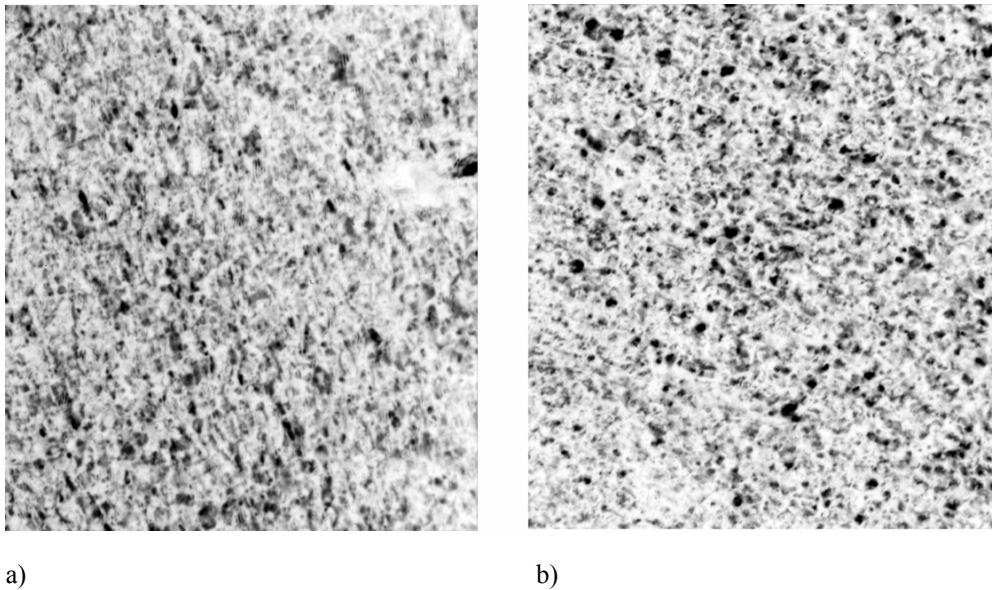


Figure 6. Microstructure observed in axial specimens of material deformed in a) compression and b) tension. Both pictures are dark field images reproduced in negative. In a) $(10\bar{1}4)$ was used for imaging and in b) $(20\bar{2}1)$ Magnification 144000x.

In both pictures it is possible to see loops clustered along certain lines, similar to the loop rafts previously reported by Jostsons et. al.[12]. However in the present case it has not been possible to associate the direction of the lines with any particular low-index direction of the lattice.

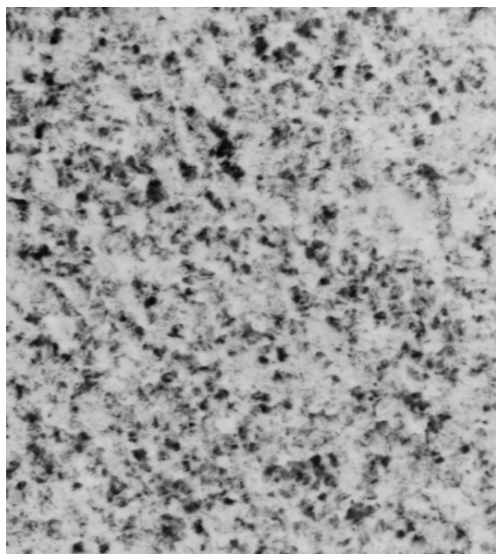


Figure 7. Dark field image of the same area as in Figure 6a using a diffraction spot from tetragonal oxide. Magnification 144000x.

Unfortunately examination of diffraction patterns showed the presence of diffraction spots which did not come from the zirconium matrix. In many cases the lattice spacing associated with these extra spots coincided with lattice spacings of the zirconium oxides or the chi (χ) hydride of zirconium [13]. As an example is shown Figure 7 which is a dark field image of the same area as in Figure 6a where a spot identified as possibly emanating from tetragonal oxide has been used for imaging. It can be assumed that all the dark spots in the figure are small crystals of

tetragonal oxide. The presence of these small oxide crystals will make the bright field images more difficult to interpret since they may be confused with the small dislocation loops observed as black dots.

In radial specimens another type of alignment of damage was occasionally observed as can be seen in Figure 8.

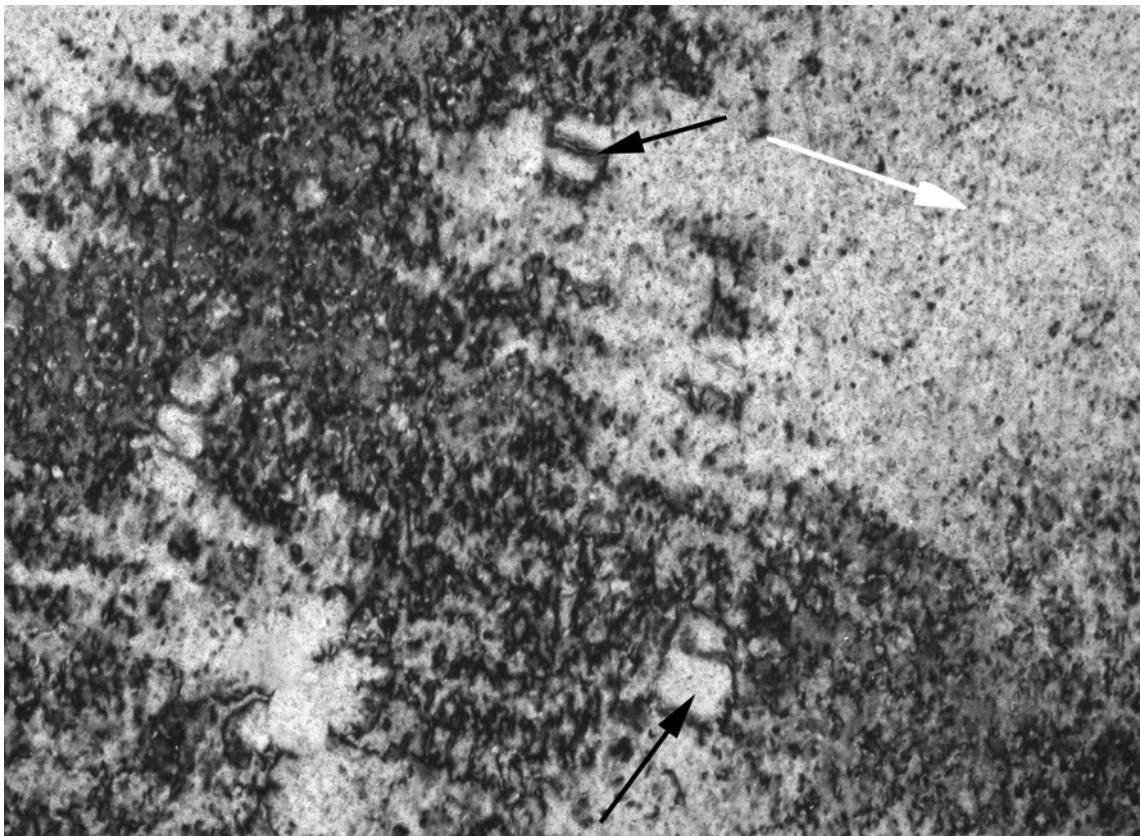


Figure 8. Damage alignment in radial specimen. The white arrow shows the $\langle 10\bar{1}0 \rangle$ - direction. The black arrows show examples of objects discussed in the text. Magnification 100000x.

The alignment seems to be in the $\langle 10\bar{1}0 \rangle$ -direction and is probably a type of corduroy effect frequently observed in irradiated Zircaloy [14]. The black arrows point to rectangular objects initially thought to be second phase particles. However microanalysis with energy dispersive X-ray spectroscopy (EDS) revealed no alloying elements at the location of the objects nor were there any extra diffraction spots detected at this location so the objects are probably not hydrides. Dark field imaging with a $(11\bar{2}2)$ -reflection showed that the boundaries of the objects lighted up. It is therefore concluded that these objects are a type of big dislocation loops, perhaps formed by the merger of a number of smaller loops, possibly as a result of the creep process.

Another observation which is not fully understood is the presence of what is probably moiré-contrast in many of the grains. The moiré-contrast is often associated with split diffraction spots.

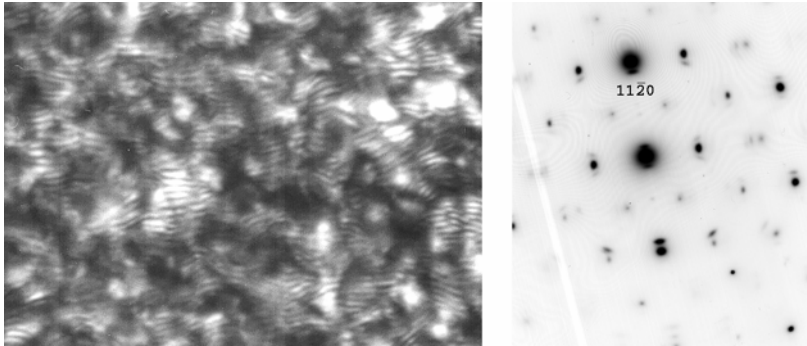


Figure 9. Moiré patterns frequently observed in connection with split diffraction spots. It is in this case the $\langle 11\bar{2}0 \rangle$ diffraction spots which are split in two. Magnification 600000x.

The obvious way of interpreting the moiré patterns is that they are caused by thin oxide crystals nucleated epitaxially on the foil surface. The slight difference in lattice constant between the oxide and the matrix then gives rise to the moiré effect. This explanation is fully consistent with the observation shown in Figure 9. The outer spots in the diffraction pattern can be interpreted as $(11\bar{2}0)$ -reflections from the zirconium matrix while the two inner spots have a spacing consistent with (200) or (112) in tetragonal oxid. The moiré spacing, about 1.5 nm is also in agreement with what would be expected if these planes have caused the effect. Similar observations were made on highly irradiated Zircaloy in a previous investigation [15] although not specifically mentioned in the report. The thing, which is difficult to understand, is that this microstructural feature is not present in unirradiated material. So probably the stress fields of the loops in some way facilitates the nucleation of the oxide crystals.

Finally it should be mentioned that no network dislocations were observed in the microstructure. If this was a result of the absence of network dislocations or a result of the masking effect of the loop structure mentioned previously can of course not be decided.

6.3 Irradiated and heat treated material

A heat treatment of irradiated material at high temperature leads to changes of the microstructure. The reason is that the mobility and equilibrium concentration of vacancies increases. Thus vacancies may be transported away from both vacancy loops and interstitial loops to other sinks for vacancies like grain boundaries. Losses of vacancies from a vacancy loop means shrinkage of the loop while an interstitial loop increases in size with emission of vacancies. Since neutral sinks like grain boundaries are not abundant in most of

the microstructure the most probable course of events is that vacancies will be both absorbed and emitted from loops so that the net result will be an overall reduction in the energy of the material. Empirically it is known that a heat treatment coarsens the loop structure. If the initial microstructure is a mixture of vacancy and interstitial loops one simple mechanism of coarsening might be that interstitial loops emit vacancies while vacancy loops absorb vacancies. The problem with such an explanation is that it leads to an increase in the dislocation line length and thus to an increase in energy. However it has been shown that vacancy and interstitial loops tend to cluster in different parts of the structure [12]. This means that for closely spaced loops of the same type larger loops might grow at the expense of smaller loops since the line energy per defect will be smaller for the large loop compared to the small loop. It is first at a later stage that interstitial and vacancy loops start to interact. And at this stage losses to grain boundaries will be relatively more important so that the net result will be that vacancy loops shrink and interstitial loops grow. Examples of coarsening of the loop structure in Zircaloy have been given by Griffiths [16]. For Zircaloy-2 irradiated at 330 K the structure consisted of 5 nm sized loops whose character could not be determined. After heat treatment for 1 h at 773 K the loops had grown to a diameter of 20-30 nm and were mostly, if not all, of interstitial character. On the other hand for a Zircaloy-4 material irradiated at 580 K the structure consisted of about 68 % vacancy loops with diameters from 10-20 nm. After annealing 1 h at 773 K the loops were mostly vacancy in character and had increased in size to 20-30 nm.

The idea behind annealing the specimens was to see if the coarser microstructure caused by the annealing would make any microstructural differences more clear between materials tested in compression or tension. The heat treatment used, 2 h at 723 K, is expected to be equivalent to 0.5 h at 773 K based on an activation energy of 1.4 eV for vacancy diffusion in Zr as given by Holt [17].

Figure 10 shows an example of the microstructure in a radial specimen of the material deformed in tension. The dark field image is taken with the $(11\bar{2}2)$ reflection so in principle all the Burgers' vectors of the **a** type should be visible. There seems to be two types of loops, one type elliptical to nearly circular and one type very elongated. One explanation to the elongated form could be that they lie on a plane very nearly parallel to the beam. That there is only one such plane of the three available possibilities can be due to the fact that the grain is oriented so that the beam makes an angle of 55° with the *c* axis. This grain is thus somewhat atypical since most grains in this orientation of the foil would make an angle of about 30° with the *c* axis. The grain is also atypical in the sense that the *c* axis is tilted in the axial direction. Now if these loops appear elongated they must be significantly larger than the other

loop population. It is in that context interesting to note that the loops are elongated in the direction of the applied stress.

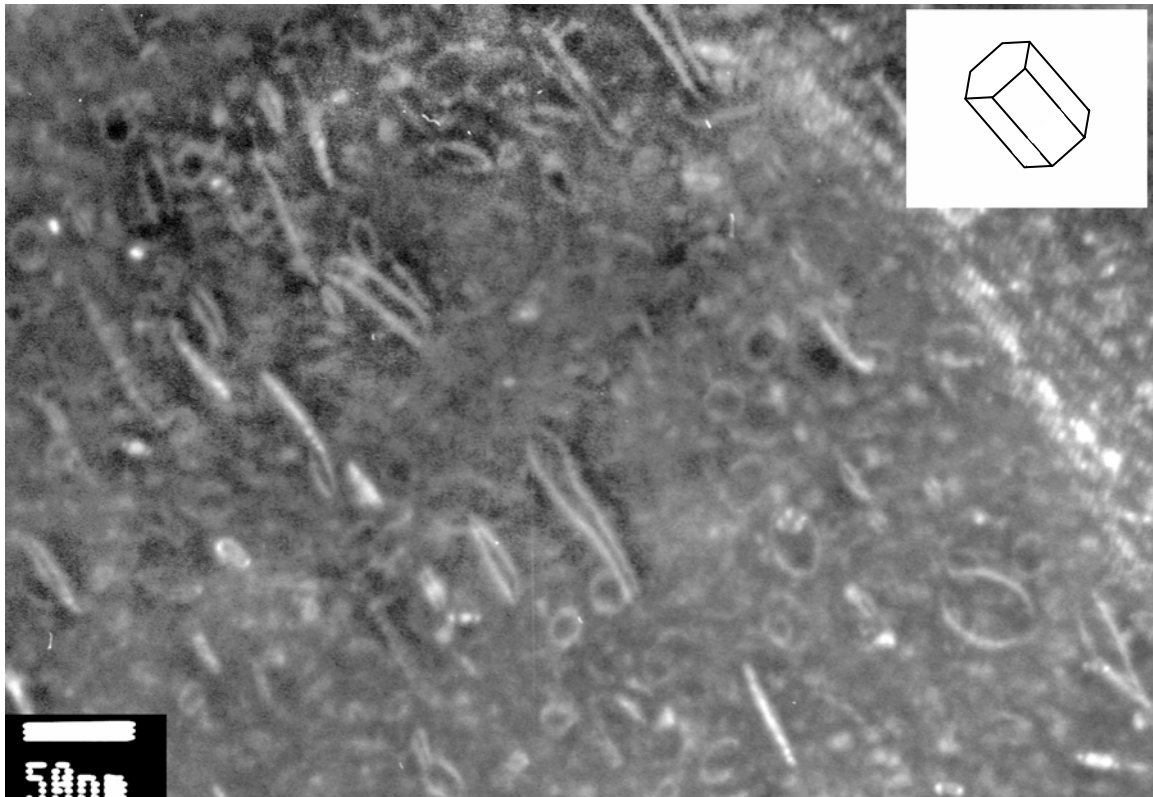


Figure 10. Loops observed with $\mathbf{g} = (11\bar{2}2)$. The insert shows the approximate orientation of the grain. The c axis projection is approximately parallel with the direction of the tensile stress. Magnification 300000x.

Figure 11 shows the microstructure of material deformed in compression. It is possible to see a dual loop size distribution, a population of large loops of about 80-100 nm in diameter and a population of smaller loops with about 20-40 nm in diameter. The large loops are elongated in a direction perpendicular to the tube wall.

In addition to the loop structure the picture contains several segments of network dislocations. Network dislocations were seen among the loop structure in almost all the grains in the heat treated material. Even if the loop structure is expected to develop into a network structure with prolonged heat treatment it is considered to be less likely that a network has started to develop at this early stage of heat treatment when most loops are still well separated from each other. It is thus concluded to be more likely that the network dislocations have been present throughout the irradiation and that the only reason why they are not observed before heat treatment is that the fine and dense loop structure formed during irradiation for some reason makes the network dislocations more or less invisible as discussed previously.

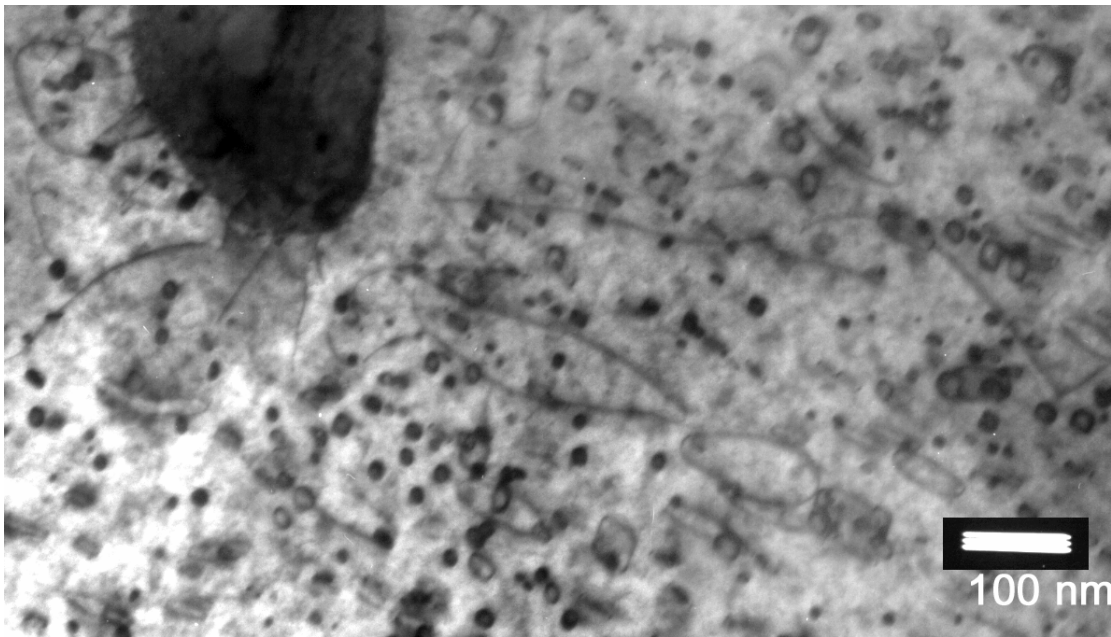


Figure 11. Microstructure in material deformed in compression. Beam direction about 22° from the basal plane. Magnification 150000x.

7. Discussion

The purpose of the present work was to determine if an examination of the microstructure in material deformed in both tension and compression might reveal important information with regard to the mechanism of irradiation creep in Zircaloy. The result is far from conclusive but the results obtained give a few indications with regard to the possible creep mechanism. With regard to the SIPA and SIPN mechanisms it seems likely that if they are at work there should be a significant difference between the microstructures deformed in tension and compression. Schematically one would expect that for a material deformed in tension along the tube axis there would be more interstitial loops than vacancy loops on planes perpendicular to the axis, and more vacancy loops than interstitial loops on planes parallel with the axis. For the material deformed in compression the opposite situation would occur. The fact that no difference in loop structures could be detected in the as-irradiated material between compression and tension materials does not prove that there is no difference in structure since the loop character was not determined. The main reasons why no character determination was attempted was lack of time (funds) and the quality of the specimens with lots of oxide crystallites on the foil surface which might create problems of correctly identifying the loops.

It was hoped that the heat treatment would reveal any differences in loop type distributions between the two types of material. One difference found is illustrated in Figures 10 and 11. In Figure 10 some of the loops are elongated in the direction of stress while in Figure 11 some of

the loops are elongated in the radial direction of the tube, i. e. perpendicular to the direction of stress. According to a review by Northwood from 1977 as cited by Griffiths [5] interstitial loops are always circular while vacancy loops are elliptical. It is therefore possible to speculate that the elongated loops are of vacancy type which is also consistent with the expected deformation under tensile and compressive stress respectively. On the other hand the orientation of the two grains in relation to the beam is such that at least one of the $\{10\bar{1}0\}$ planes must be parallel with the beam which would make even circular loops appear elongated.

More important perhaps is the observation that there is a density of network dislocations in the heat treated material. This makes it probable that these dislocations are also present in the as-irradiated material and that it is the motion of these dislocations that are responsible for the observed irradiation creep. In the previous analysis of the in-pile creep experiment it was concluded that the creep in the bent rod was still in the primary stage of irradiation creep [3]. This conclusion was based on a comparison of the R2 data with a larger data base on measurements of creep down of empty cladding tubes [4]. In the diagram below it is quite clear that the R2 data fall in the primary stage of the general creep trends.

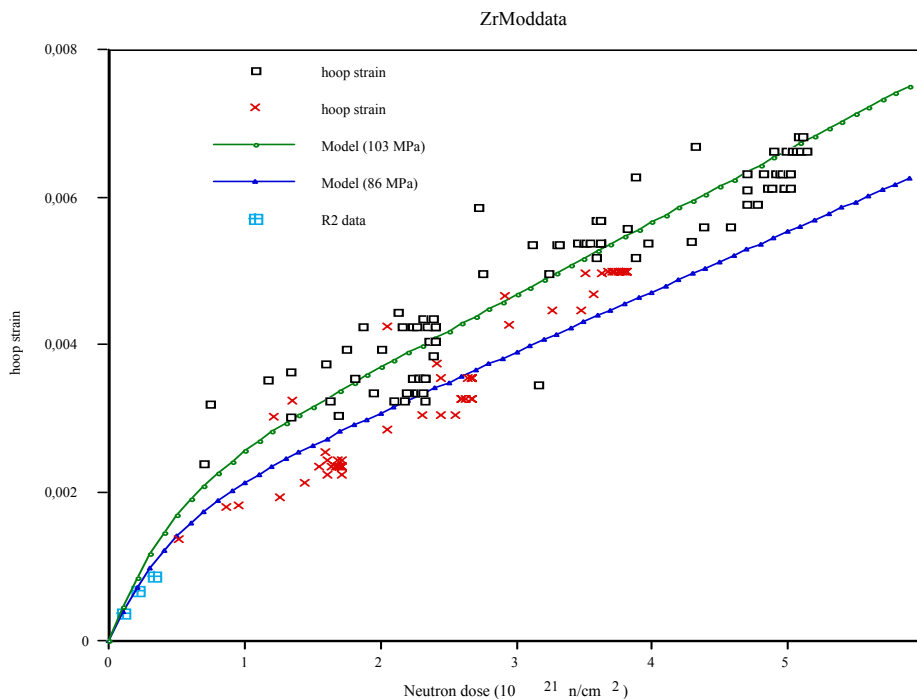


Figure 12. The R2 creep data plotted with the data base of clad creep down data from [4]

Note that this irradiation primary creep is some other phenomenon than the normal primary creep observed in the unirradiated control specimen shown in Figure 3. On the basis of the observed behaviour of the in-pile creep of Zircaloy and the microstructural observations it is reasonable to conclude that the mechanism for in-pile creep in Zircaloy is irradiation

enhanced climb passed obstacles where a net climb is caused by slightly more interstitials than vacancies being absorbed by dislocations.

Initially the existing dislocations in the material glide up against the obstacles which control the yield strength in unirradiated Zircaloy. These obstacles are most probably oxygen atoms since it is known that oxygen works as a solid solution strengthener of Zircaloy. If there is no irradiation this glide causes the transient deformation seen for the unirradiated material in Figure 3. In the absence of irradiation no further plastic deformation occurs if the stress remains constant. However once irradiation starts climb will help the dislocations to pass the relatively short range obstacles of oxygen atoms. But the irradiation also results in the formation of vacancy and interstitial loops which also function as obstacles to dislocation glide. The loops are also stronger obstacles than the oxygen atoms but still passable by climb even if it takes longer. Thus deformation will continue but the rate will be decreased as long as the density of loops increases. Eventually the loop density saturates and then the creep rate will be constant. Note that the start of the secondary stage in Figure 12 at about 10^{21} n/cm² agrees well with the irradiation doses when the loop density saturates.

The secondary stage in Figure 12 is not necessarily a steady state deformation. With the present model for irradiation creep the dislocation glide will by necessity lead to an increase in the dislocation density. There will thus be some strain hardening. However in comparison with many other metals the strain hardening in Zircaloy is fairly low. It should also be noted that the range of strain covered in Figure 12 is only 0.007. In this range of strain only a minor amount of strain hardening will occur and therefore the creep rate can appear to be constant even if that is not strictly true, especially since there is such a large amount of scatter in the creep data.

8. Conclusions

- There is no easily detectable difference in the microstructure between materials creep deformed in-pile in tension or compression.
- After a heat treatment to coarsen the irradiation induced microstructure there are still no easily detectable differences between the two types of material.
- After heat treatment network dislocations become visible. It is probable that these dislocations are also present in the as-irradiated material.
- Based on these observations it is concluded that the mechanism of irradiation creep is irradiation enhanced climb passed obstacles. In the primary stage the density of loops

increases which leads to a decrease of the creep rate. When the loop density saturates a quasi steady-state creep deformation takes place.

9. References

1. Pettersson, K.
Irradiation creep of zirconium alloys at high neutron fluences – an assessment of the state-of-the-art. Department of Materials Science and Engineering, KTH, Stockholm, 1997-03-03
2. Tomani, H. and Lindelöw, U.
In-pile creep tests of Zircaloy tubing in the Studsvik R2 reactor. Final Report Studsvik Nuclear, SKI Report 99:41, December 2000
3. Pettersson, K.
Evaluation of results from an In-pile creep test in the Studsvik R2 reactor KTH- Materials Science and Engineering, SKI Report 02:48, Stockholm, January 2002
4. Franklin, D.G., Lucas, G.E., and Bement, A.L.,
Creep of Zirconium alloys in nuclear reactors. ASTM STP 815. 1983, Philadelphia: American Society for Testing and Materials.
5. Griffiths, M.
A review of microstructure evolution in zirconium alloys during irradiation. Journal of Nuclear Materials, 1988. **159**: p. 192-218.
6. Gittus, J.H.
Theory of dislocation-creep due to the Frenkel defects or interstitialcies produced by bombardement with energetic particles. Philosophical Magazine, 1972. **25**: p. 345-354.
7. Dollins, C.C. and Nichols, F.A.
Mechanisms of irradiation creep in zirconium-base alloys. in *Zirconium in Nuclear Applications.* 1974. Portland, Or.: ASTM.229-248
8. Baty, D.L. et. al.
Deformation characteristics of cold-worked and recrystallized Zircaloy-4 cladding. in *"Zirconium in the Nuclear Industry: Sixth Int. Symp.* 1984: American Society for Testing and Materials.306-339
9. Pettersson, K.
Unpublished results. 1975.
10. Carpenter, G.J.
Electron irradiation damage in zirconium and Zircaloy-2 in a high voltage electron microscope. in *6th European Congress on Electron Microscopy.* 1976. Jerusalem.556-558
11. Northwood, D.et.al.
Characterization of neutron irradiation damage in zirconium alloys - an international "round-robin" experiment. Journal of Nuclear Materials, 1979. **79**: p. 379-394.

12. Jostsons, A., et al.
Neutron irradiation-induced defect structures in zirconium. in *Effects of radiation on structural materials.* 1979: ASTM.62-76
13. Chung, H.
Phase transformations in neutron-irradiated Zircalloys. in *Effects of Radiation on Materials: 13th International Symposium (Part 1).* 1987: ASTM.676-699
14. Kelly, P.M., Blake, R. G., Jostsons, A.
An interpretation of Corduroy contrast in neutron irradiated zirconium. Journal of Nuclear Materials, 1976. **59**: p. 307-315.
15. Pettersson, K.
Characterization of the Microstructure in Recrystallized Zircaloy-2 Cladding Irradiated to a High Neutron Dose SKI, SKI Report 2003:33, Stockholm
16. Griffiths, M.
A review of microstructure evolution in zirconium alloys during irradiation. Journal of Nuclear Materials, 1988. **159**: p. 190-218.
17. Holt, R.A.
Mechanisms of irradiation growth of alpha-zirconium alloys. Journal of Nuclear Materials, 1988. **159**: p. 310-338.

www.ski.se

STATENS KÄRNKRAFTINSPEKTION
Swedish Nuclear Power Inspectorate

POST/POSTAL ADDRESS SE-106 58 Stockholm

BESÖK/OFFICE Klarabergsviadukten 90

TELEFON/TELEPHONE +46 (0)8 698 84 00

TELEFAX +46 (0)8 661 90 86

E-POST/E-MAIL ski@ski.se

WEBBPLATS/WEB SITE www.ski.se